Supplementary Information for

Fe-modified CoCr layered double hydroxide for boosting seawater oxygen evolution reaction

Edmond Nasr, Paul Byaruhanga, Dezhi Wang, Shuo Chen, Luo Yu,*, and Zhifeng Ren*

Department of Physics and Texas Center for Superconductivity at the University of Houston (TcSUH), University of Houston, Houston, Texas 77204, USA.

* Corresponding author.

E-mail: lyu2@central.uh.edu (L. Yu); zren@uh.edu (Z. F. R.)

Experimental section

Materials and chemicals. 2-methylimidazole ($C_4H_6N_2$, 99%, Sigma Aldrich), cobalt (II) nitrate hexahydrate [$Co(NO_3)_2 \cdot 6H_2O$, Sigma Aldrich], iron (II) sulfate heptahydrate ($FeSO_4 \cdot 7H_2O$, Sigma Aldrich), chromium (III) nitrate nonahydrate [$Cr(NO_3)_3 \cdot 9H_2O$, Sigma Aldrich], nickel (II) nitrate hexahydrate [$Ni(NO_3)_2 \cdot 6H_2O$, Sigma Aldrich], ammonium molybdate tetrahydrate [$(NH_4)_6Mo_7O_{24} \cdot 4H_2O$, Sigma Aldrich], urea ($CH_4N_2O$, Promega Corporation), potassium hydroxide (KOH, Alfa Aesar), ethanol (CH_3CH_2OH, Koptec), hydrochloric acid (HCL, RICCA Chemical Company), and nickel foam (thickness: 1.6 mm) were used without further purification and deionized (DI) water was used for all aqueous solutions.

Materials synthesis. Fe-CoCr LDH was synthesized using a previously reported Co MOFs precursor.[1,2] First, a piece of Ni foam (2 cm × 5 cm) was ultrasonicated sequentially in 3 M HCl, ethanol, and DI water for 5 minutes each to remove surface impurities. To prepare the Co MOFs on the Ni foam, two aqueous solutions were prepared: Solution A contained 40 mL of 0.04 M $Co(NO_3)_2 \cdot 6H_2O$ and 0.01 M $Ni(NO_3)_2 \cdot 6H_2O$, and Solution B contained 40 mL of 0.4 M 2-methylimidazole ($C_4H_6N_2$). Solution B was rapidly added to Solution A under stirring, and the pre-cleaned Ni foam substrate was immediately immersed into the resulting mixture. After a 4-hour reaction at room temperature, the sample was removed, rinsed with DI water, and dried at room temperature overnight. A small section (1 cm × 2 cm) of the resulting Co MOFs-coated Ni foam was then immersed in 10 mL of a mixed aqueous solution containing 0.15 M $FeSO_4 \cdot 7H_2O$ and 0.15 M $Cr(NO_3)_3 \cdot 9H_2O$. After 1 hour of soaking, the modified sample was removed from the solution, washed with DI water, and dried overnight, yielding the final Fe-CoCr LDH. The transformation follows an etching-incorporation-sedimentation mechanism that is further discussed in the Catalyst synthesis and characterization section in the main text.[3,4]

To prepare the benchmark IrO_2 on Ni foam electrode, 40 mg of commercial IrO_2 and 60 μL of Nafion were dispersed in a mixture of 540 μL ethanol and 400 μL DI water in a 2 mL tube.[5] The

mixture was ultrasonicated for 30 minutes, after which a piece of Ni foam (~2 cm^2) was placed into the tube and gently swayed several times to ensure even coating. The Ni foam was then soaked in the dispersion, removed, and air-dried overnight.

To synthesize NiMoN as the HER counterpart for overall water splitting, we adopted a previously reported method using Ni foam as the substrate. First, $NiMoO_4 \cdot xH_2O$ was prepared as a precursor.[6] A piece of Ni foam (1.5 cm × 2.5 cm) was cleaned by sequential ultrasonication in 3 M HCl, ethanol, and DI water for 5 minutes each. In parallel, an aqueous solution was prepared by dissolving 2 mmol of $Ni(NO_3)_2 \cdot 6H_2O$, 0.25 mmol of $(NH_4)_6Mo_7O_{24} \cdot 4H_2O$, and 3 mmol of urea in 20 mL of DI water. The pretreated Ni foam was immersed in this solution, and the mixture was placed in a water bath oven at 90 °C for 8 hours. After the reaction, the sample was rinsed thoroughly with DI water and dried in air, yielding a light green $NiMoO_4 \cdot xH_2O$-coated Ni foam. To convert this precursor to NiMoN, an ammonia-assisted reduction was carried out. The $NiMoO_4 \cdot xH_2O$ sample was placed in the center of a quartz tube in a furnace and annealed at 400 °C for 2 hours under a gas flow consisting of ammonia (120 sccm) and argon (60 sccm), with a ramp rate of 10 °C/min. In this step, ammonia functioned as both the reducing agent and the nitrogen source. After natural cooling, the resulting black product was designated as NiMoN.

Structural characterization. The phase and crystal structure of the obtained Fe-CoCr LDH on Ni foam were characterized by X-ray diffraction (XRD, Rigaku SmartLab). The microstructure and elemental composition were examined using scanning electron microscopy (SEM, JEOL JSM-6330F) and transmission electron microscopy (TEM, JEOL JEM-2010F), including energy-dispersive X-ray spectroscopy (TEM-EDS) analysis. The surface oxidation states of the constituent elements were analyzed by X-ray photoelectron spectroscopy (XPS, PHI Quantera).

Electrochemical characterization. Electrochemical measurements were conducted using a Gamry Reference 3000 electrochemical workstation. The OER performance was evaluated in a three-electrode system with 1.0 M KOH as the electrolyte. A graphite rod, a Hg/HgO electrode, and Fe-CoCr LDH on Ni foam served as the counter electrode, the reference, and the working electrode, respectively. All potentials were converted to the reversible hydrogen electrode (RHE) scale using the Nernst equation:

$$E_{RHE} = E_{Hg/HgO} + 0.098 + 0.0591 \times pH.$$

Cyclic voltammetry (CV) was performed at a scan rate of 2 mV s^{-1} with iR compensation applied. The reverse scan of each CV curve was reported as the respective OER polarization curve. Current densities were normalized to the geometric area of the Ni foam. Overpotentials (η) were calculated using the equation:

$$\eta\ (V) = E_{RHE} - 1.23\ V.$$

Tafel slopes were derived from the Tafel equation:

$$\eta = a + b \log(j),$$

where b is the Tafel slope, j is the current density, and a is the y-intercept. The electrochemical surface area (ECSA) was estimated by determining the double-layer capacitance C_{dl} in the non-faradaic region. CV measurements were performed at scan rates from 20 to 100 mV s^{-1} within a potential range of 0.72 to 0.82 V *vs.* RHE. A plot of capacitive current versus scan rate yielded C_{dl} as half the slope. The ECSA was then calculated using: $ECSA = C_{dl}/C_S$ where C_S is the specific capacitance of a flat surface.

Electrochemical impedance spectroscopy (EIS) was conducted at an overpotential of 300 mV over a frequency range of 0.01 Hz to 100 kHz with a 10 mV AC amplitude.

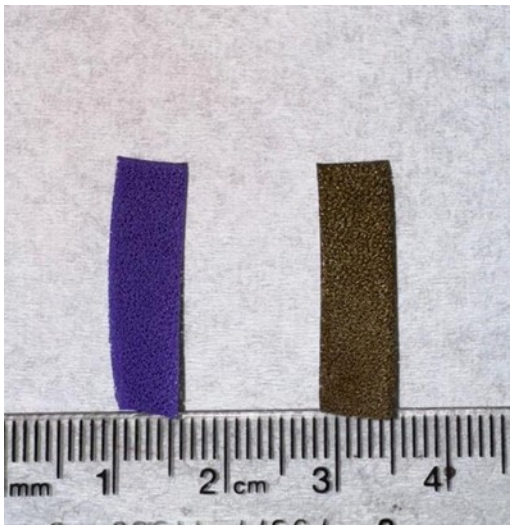

Fig. S1. Optical images of Co MOFs (left) and Fe-CoCr LDH (right).

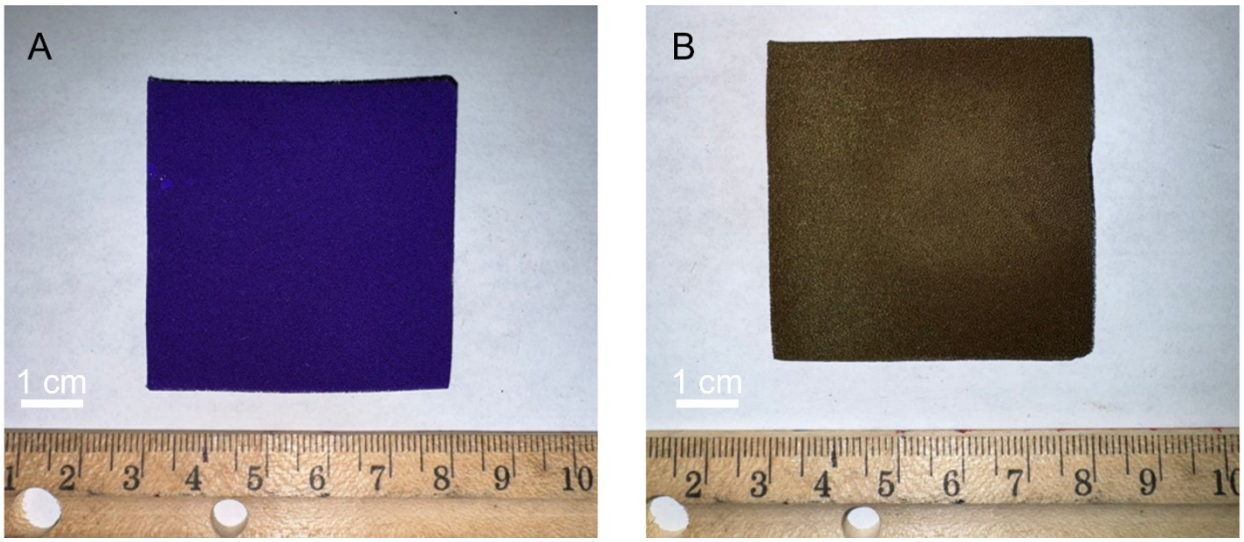

Fig. S2. Optical images of (A) Co MOFs and (B) Fe-CoCr LDH synthesized on Ni foam of 5 cm × 5 cm.

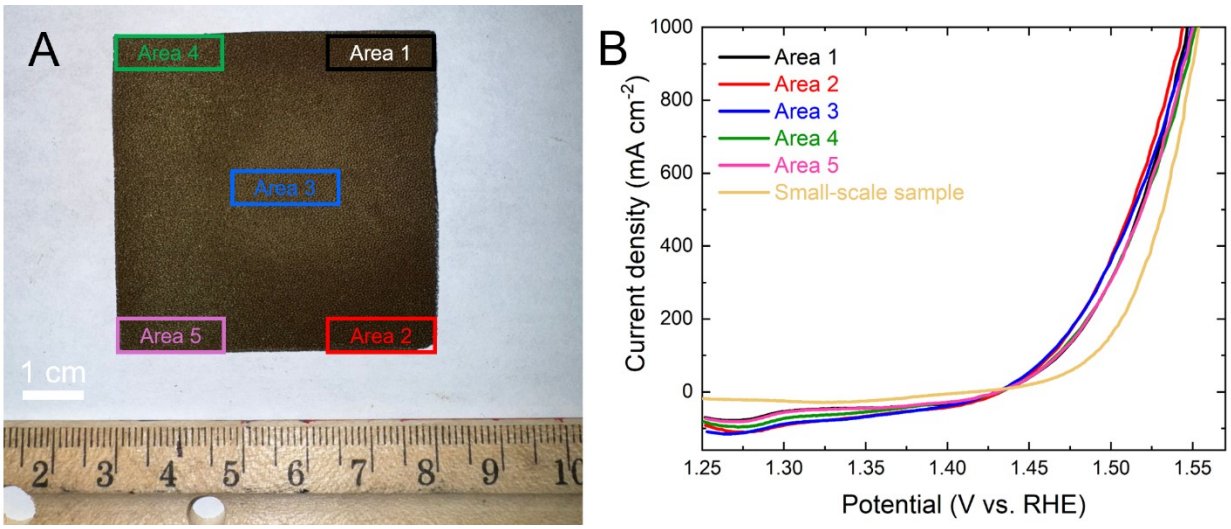

Fig. S3. (A) Optical images of Fe-CoCr LDH synthesized on Ni foam of 5 cm × 5 cm and (B) OER polarization curves measured from five different areas cut from the large electrode and compared to the small-scale sample.

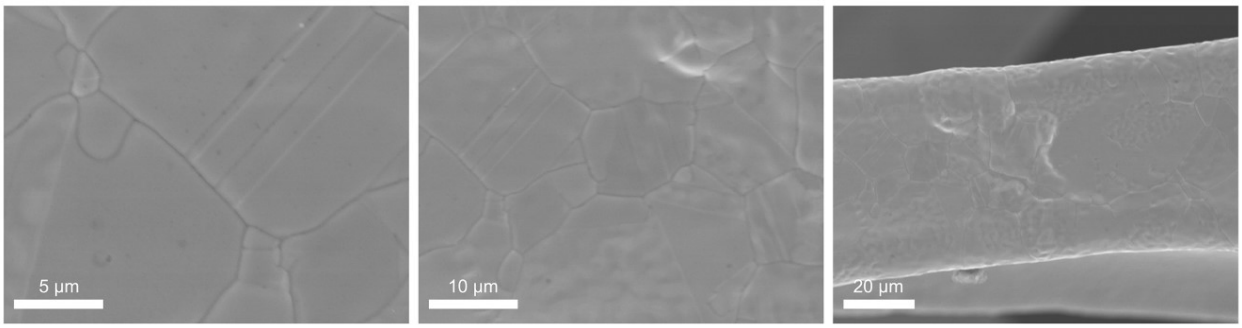

Fig. S4. SEM images of bare Ni foam.

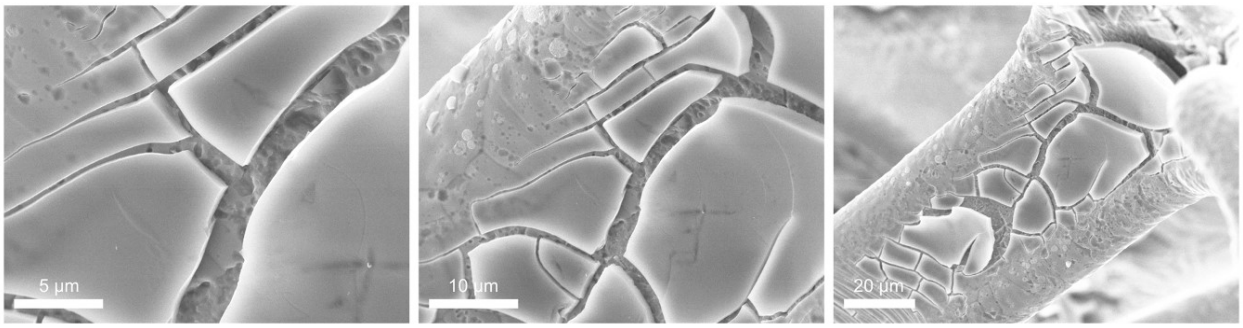

Fig. S5. SEM images of CoCr LDH.

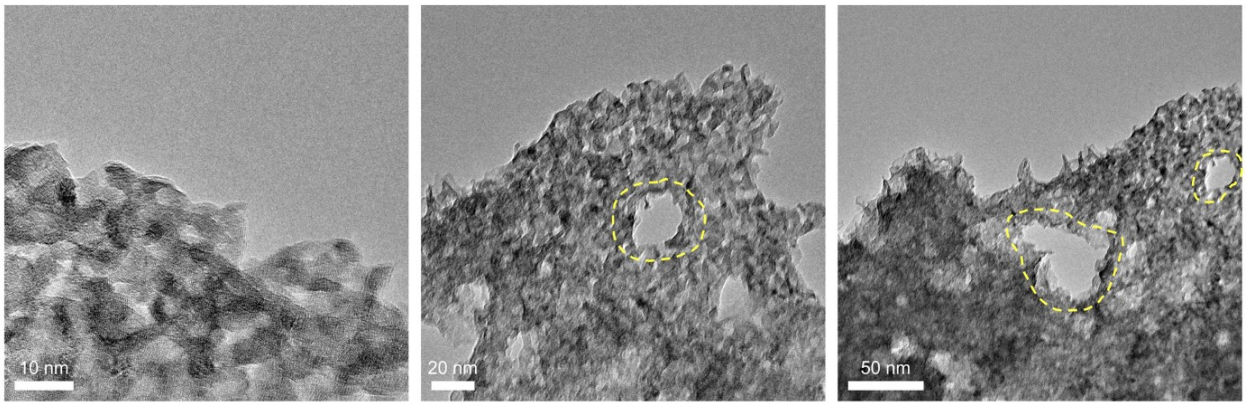

Fig. S6. HRTEM and TEM images of Fe-CoCr LDH.

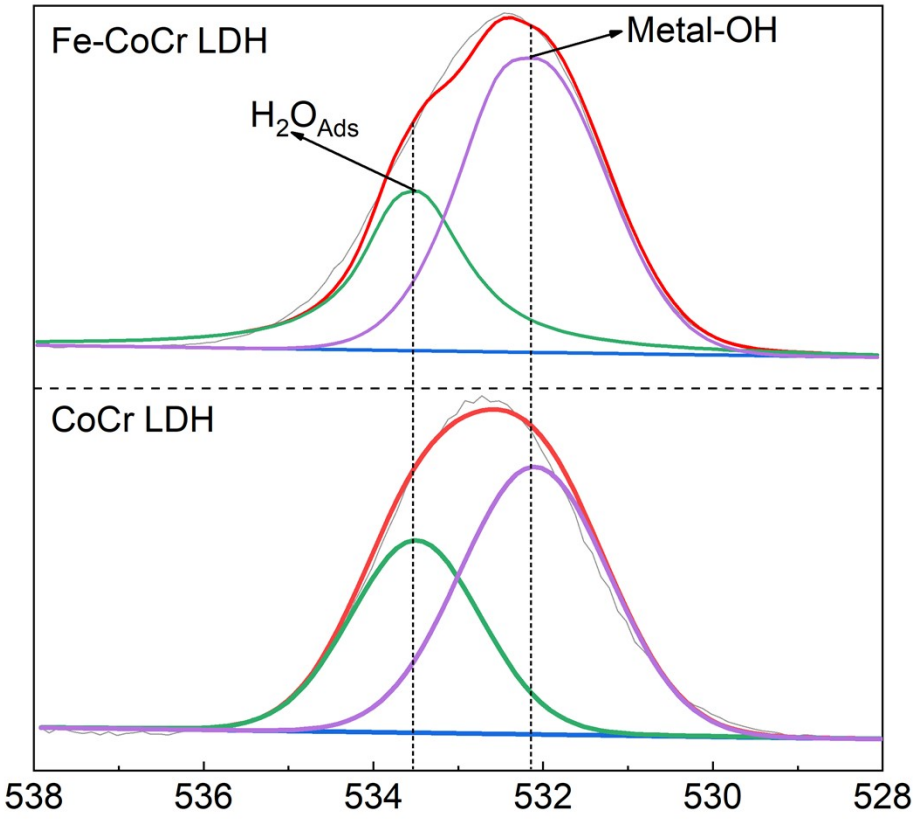

Fig. S7. High-resolution XPS of O 1s for CoCr LDH and Fe-CoCr LDH.

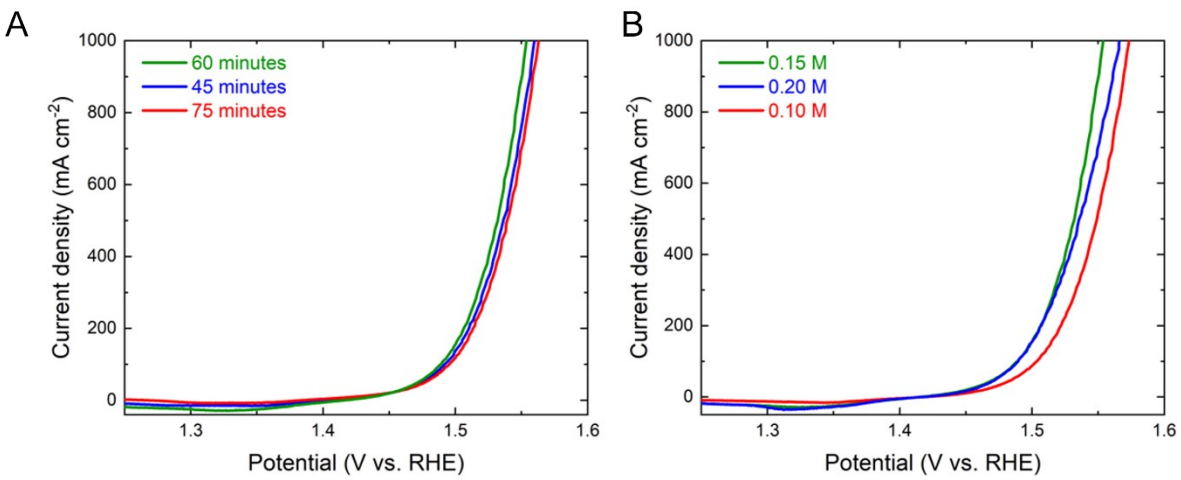

Fig. S8. OER polarization curves of Fe-CoCr LDH prepared with (A) varying second-step reaction times and (B) $FeSO_4 \cdot 7H_2O$ concentrations in the second step.

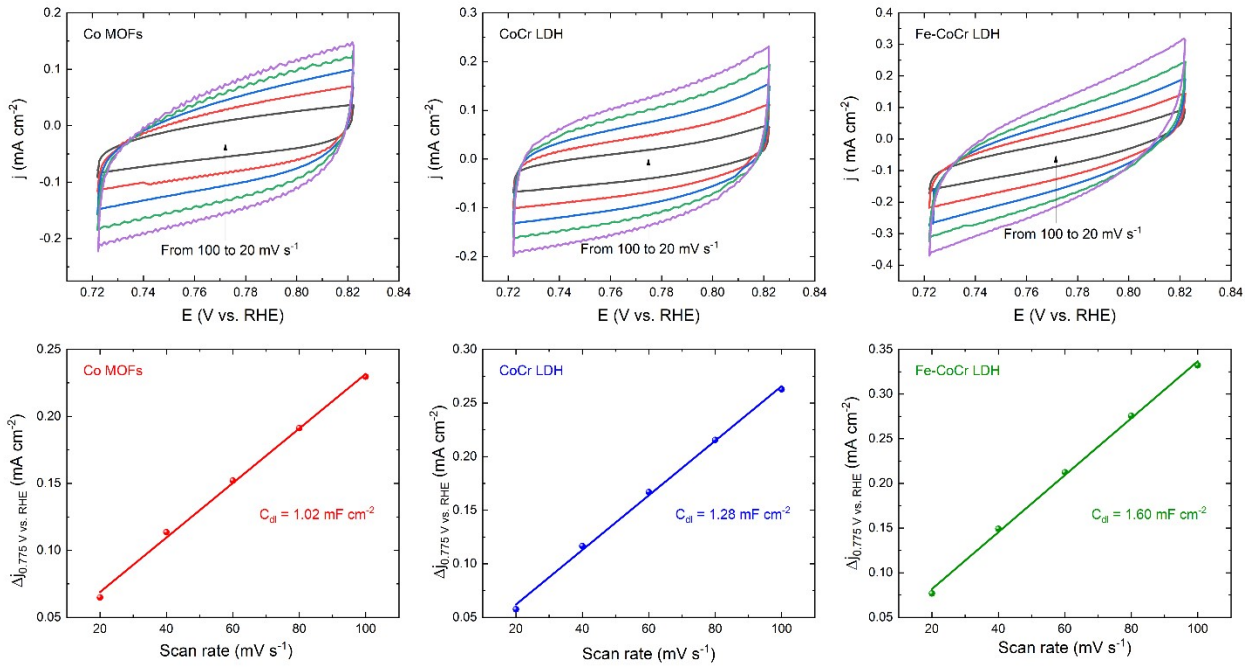

Fig. S9. Cyclic voltammetry curves recorded at various scan rates in the non-faradaic potential region (top) and corresponding plots of capacitive current *vs.* scan rate (bottom) for Co MOFs, CoCr LDH, and Fe-CoCr LDH. The slope of the linear fit represents twice the double-layer capacitance, and C_{dl} is determined by dividing the slope by two. The C_{dl} values are then used to estimate the electrochemical active surface area (ECSA) of each sample, as shown in detail below.

Calculation of ECSA for each catalyst:

$ECSA = \frac{C_{dl}}{C_S}; C_S = 40\ \mu F\ cm^{-2}$ is the specific capacitance for a flat surface.[7,8]

$$ECSA_{Co\ MOFs} = \frac{1.02\ mF\ cm^{-2}}{40\ \mu F\ cm^{-2}} = 25.5\ cm^2$$

$$ECSA_{CoCr\ LDH} = \frac{1.28\ mF\ cm^{-2}}{40\ \mu F\ cm^{-2}} = 31.25\ cm^2$$

$$ECSA_{Fe-CoCr\ LDH} = \frac{1.60\ mF\ cm^{-2}}{40\ \mu F\ cm^{-2}} = 40\ cm^2$$

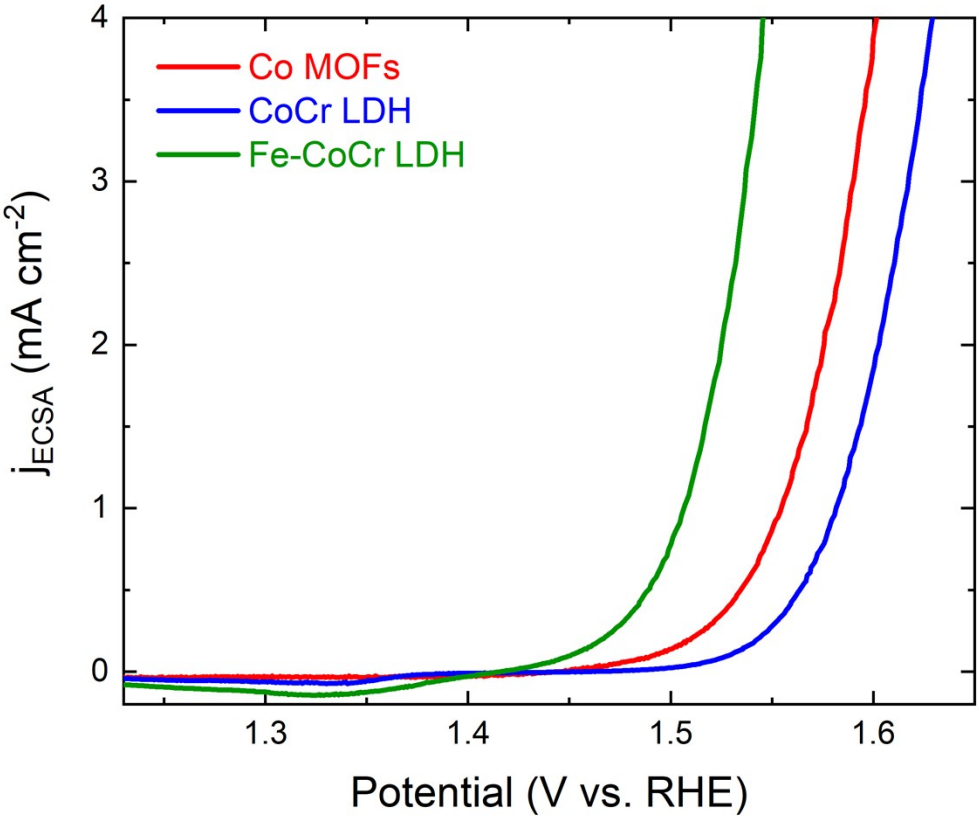

Fig. S10. ECSA-normalized polarization curves for Co MOFs, CoCr LDH, and Fe-CoCr LDH.

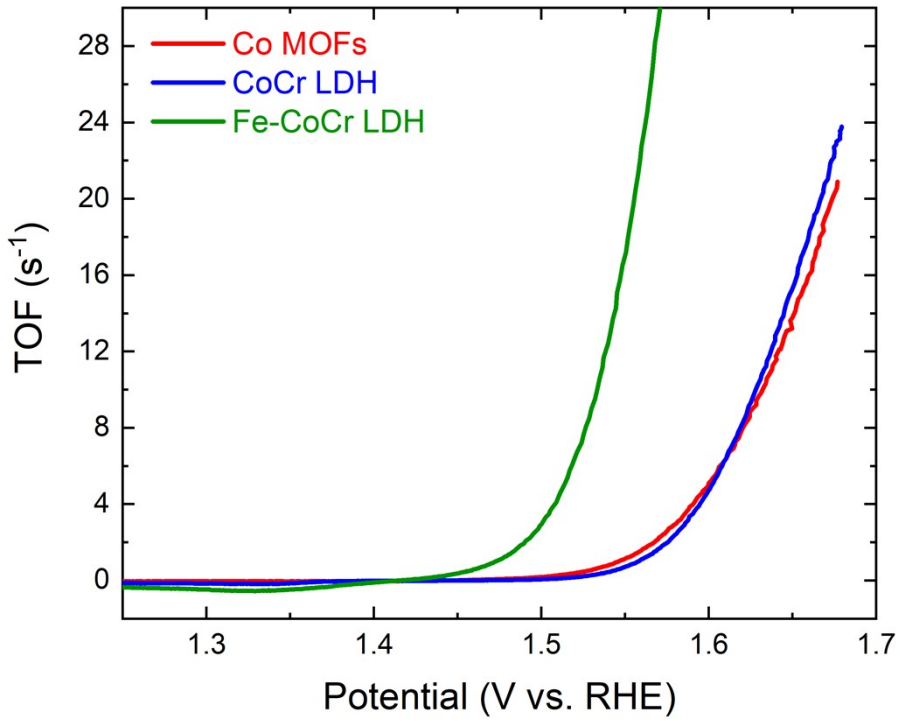

Fig. S11. TOF plots of Co MOFs, CoCr LDH, and Fe-CoCr LDH.

The calculation of the number of active sites per cm^2, estimated from the double-layer capacitance (C_{dl}), is essential for determining the turnover frequency (TOF) which is given by the following equation: $TOF = \frac{j \times N_A}{4 \times F \times n_{sites}}$ where j is the current density in A/cm^2, N_A is Avogadro's number, F is Faraday's constant and n_{sites} is the number of surface sites/cm^2. In this work, a specific capacitance value of 40 µF cm^{-2} was assumed for a flat electrode, consistent with previous reports.[7] Additionally, a surface site density of 2×10^{15} sites cm^{-2} for the flat standard electrode was used as the reference for our calculations.[8]

Thus, the number of active sites for each catalyst was calculated as follows:

Co MOFs:

$$\frac{1.02\ mF\ cm^{-2}}{40\ \mu F\ cm^{-2}} \times 2 \times 10^{15}\ surface\ sites/cm^2 = 5.1 \times 10^{16} surface\ sites/cm^2$$

CoCr LDH:

$$\frac{1.28\ mF\ cm^{-2}}{40\ \mu F\ cm^{-2}} \times 2 \times 10^{15}\ surface\ sites/cm^2 = 6.4\ \times 10^{16} surface\ sites/cm^2$$

Fe-CoCr LDH:

$$\frac{1.60\ mF\ cm^{-2}}{40\ \mu F\ cm^{-2}} \times 2 \times 10^{15}\ surface\ sites/cm^2 = 8\ \times 10^{16} surface\ sites/cm^2$$

And then after converting into mol, the final TOF was calculated as follows:

Co MOFs:

$$\frac{6.02 \times 10^{23}}{5.1 \times 10^{16} \times 4 \times 9.6485 \times 10^{4}} \times j \times 10^{-3} = 0.031\ j\ s^{-1}$$

CoCr LDH:

$$\frac{6.02 \times 10^{23}}{6.4 \times 10^{16} \times 4 \times 9.6485 \times 10^{4}} \times j \times 10^{-3} = 0.024\ j\ s^{-1}$$

Fe-CoCr LDH:

$$\frac{6.02 \times 10^{23}}{8 \times 10^{16} \times 4 \times 9.6485 \times 10^{4}} \times j \times 10^{-3} = 0.019\ j\ s^{-1}$$

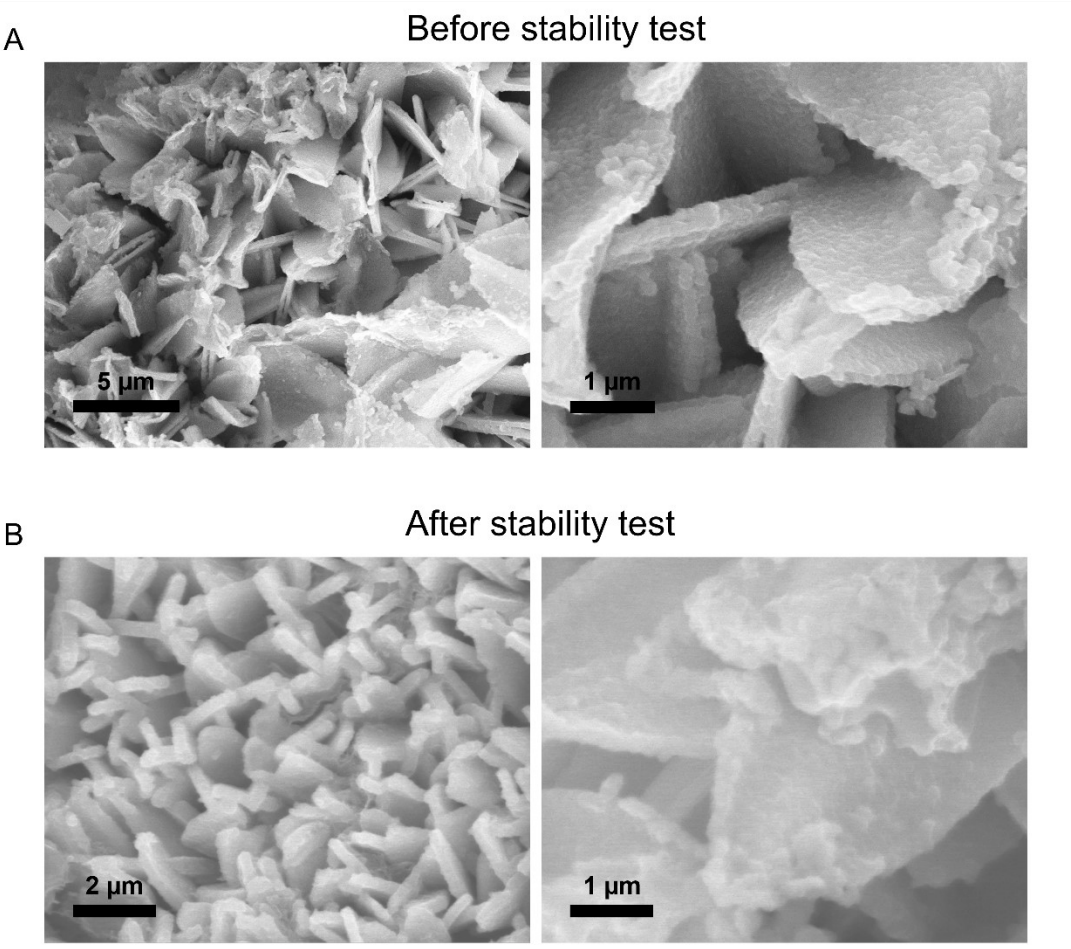

Fig. S12. SEM images of Fe-CoCr LDH (A) before and (B) after stability testing in 1 M KOH + Natural Seawater electrolyte.

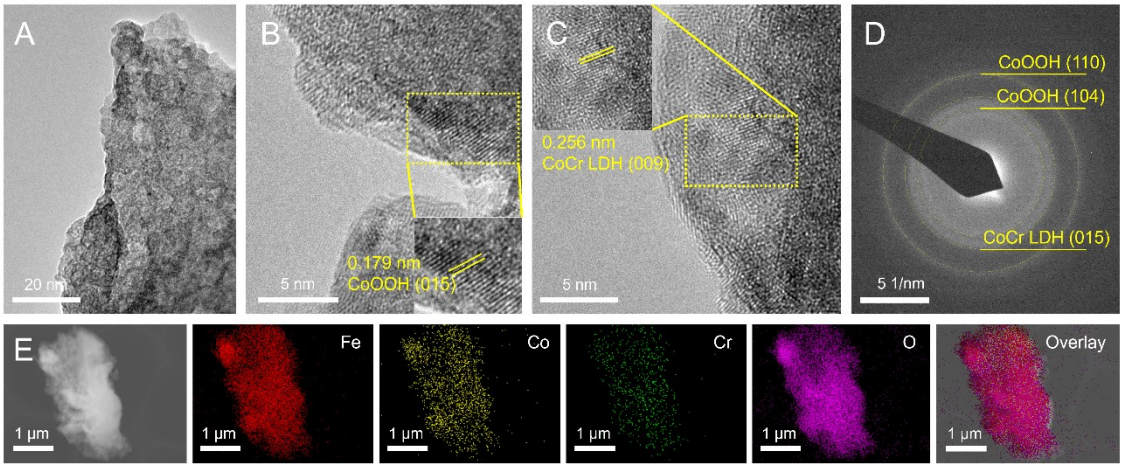

Fig. S13. (A) TEM, (B and C) HRTEM images, (D) SAED pattern, and (E) ADF-STEM image and corresponding elemental mapping images for Fe-CoCr LDH after OER stability testing in 1 M KOH + Natural Seawater.

To provide further insight on structural stability, we conducted TEM, HRTEM, SAED, and ADF-STEM with elemental mapping on the Fe-CoCr LDH catalyst after OER stability testing in seawater. As the results shown above, HRTEM revealed lattice fringes with d-spacings of 0.256 nm and 0.179 nm, assigned to the (009) plane of CoCr LDH and the (015) plane of CoOOH, respectively. Correspondingly, SAED patterns displayed three distinct rings with measured d-spacings of 0.141 nm, 0.191 nm, indexed to the (110) and (104) planes of CoOOH, respectively, and 0.229 nm, indexed for the (015) plane of CoCr LDH. Finally, ADF-STEM imaging and elemental mapping confirmed the uniform distribution of Fe, Co, Cr, and O throughout the nanosheets.

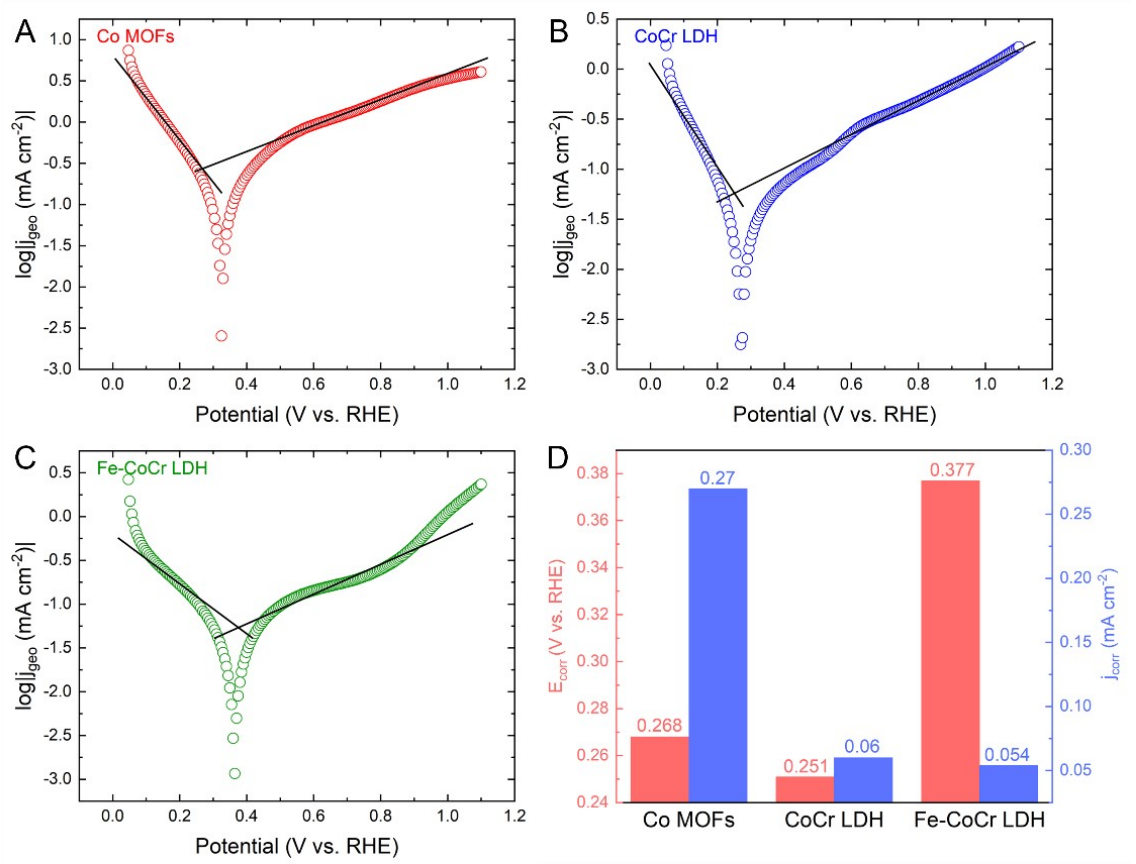

Fig. S14. Corrosion polarization curves of (A) Co MOFs, (B) CoCr LDH, (C) Fe-CoCr LDH, and (D) Column graph to summarize the data.

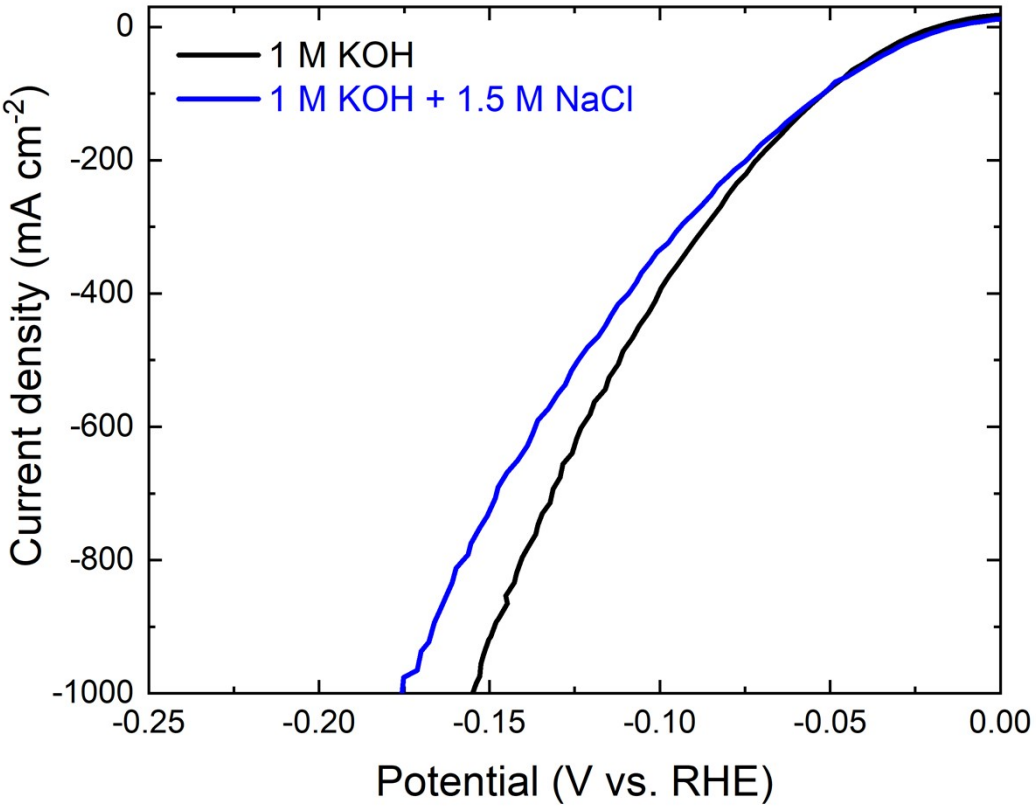

Fig. S15. HER polarization curves for NiMoN in 1 M KOH and 1 M KOH + 1.5 M NaCl.

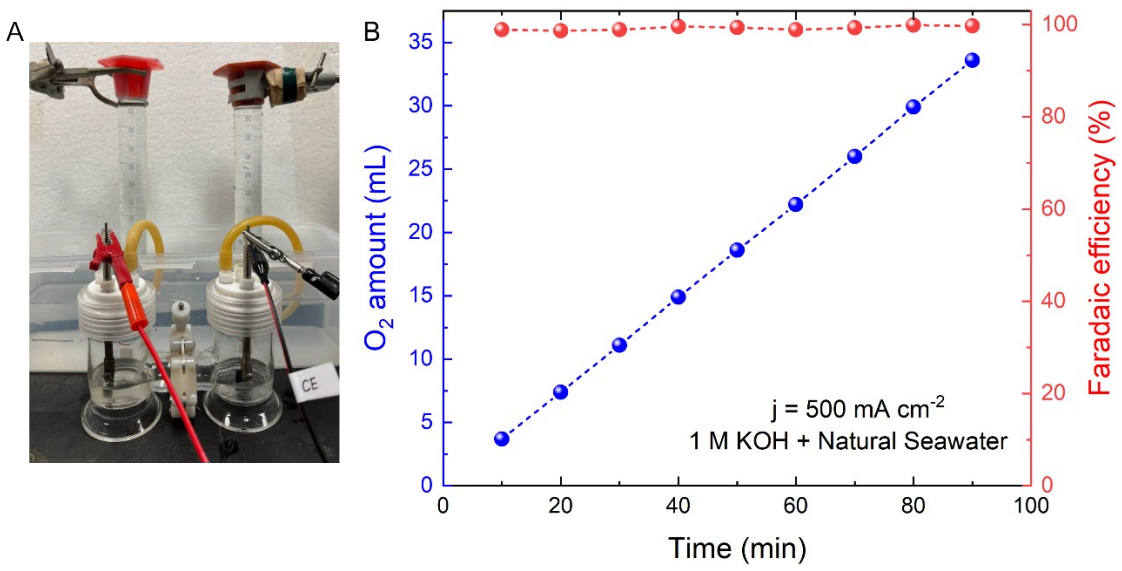

Fig. S16. Experimental measurements of O_2 gas amounts produced by our water electrolyzer. (A) Optical image of the H-cell supported drainage set-up. (B) Faradaic efficiency of Fe-CoCr LDH measured at 500 mA cm^{-2} for O_2 evolution.

Fig. S17. Hypochlorite detection result for the electrolyte after 1.5 h seawater electrolysis at 500 mA cm^{-2}.

To verify whether hypochlorite was generated during seawater electrolysis, we employed a chlorine (hypochlorite) visual test kit (CHEMetrics K-5808, see details at https://www.chemetrics.com/product/k-5808/). The test is based on the oxidation of N,N-diethyl-p-phenylenediamine (DPD), which produces a pink-colored species in proportion to the chlorine concentration. Free chlorine is detected directly, while total chlorine (free chlorine + chloramines) is determined by the addition of potassium iodide, which is first oxidized to iodine; the iodine then oxidizes DPD to form the same pink species. After 1.5 h of electrolysis at 500 mA cm^{-2} in alkaline natural seawater, the test ampoule (Fig. S12) remained completely transparent without any pink coloration. This result confirms that no hypochlorite was generated in the electrolyte, indicating that chlorine evolution did not occur on the anode.

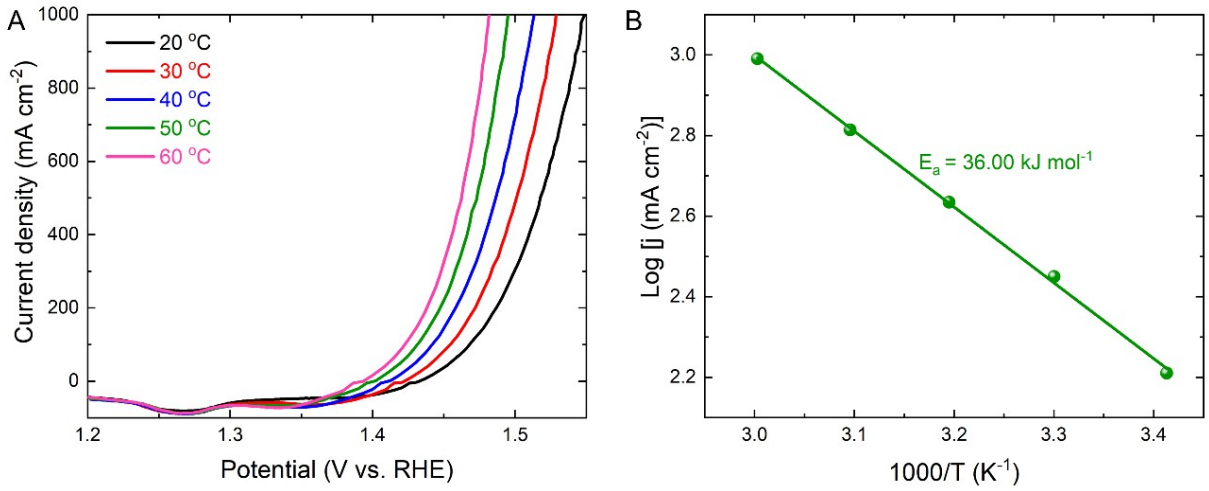

Fig. S18. (A) OER polarization curves of Fe-CoCr LDH measured at different temperatures in 1 M KOH and (B) Arrhenius plot of Fe-CoCr LDH in 1 M KOH.

The following Arrhenius equation was used to calculate the electrochemical activation energy, E_a in kJ mol^{-1}, for OER catalysts:[9]

$$j = e^{\frac{-E_a}{2.303RT}}$$

$$\log(j) = \frac{-E_a}{2.303RT}$$

$$\frac{\partial\{\log(j)\}}{\partial\left(\frac{1}{T}\right)} = \frac{-E_a}{2.303R}$$

Where j is the current density in mA cm^{-2} at a given potential, T is the temperature in K, and R is the gas constant given by R = 8.3145 J mol^{-1} K^{-1}.

1 N. Cheng, L. Ren, X. Xu, Y. Du and S. X. Dou, *Adv. Energy Mater.*, 2018, **8**, 1801257.

2 W. Cheng, Z. P. Wu, D. Luan, S. Q. Zang and X. W. Lou, *Angew. Chem., Int. Ed.*, 2021, **60**, 26397–26402.

3 K. Zhu, J. Chen, W. Wang, J. Liao, J. Dong, M. O. L. Chee, N. Wang, P. Dong, P. M. Ajayan, S. Gao, J. Shen and M. Ye, *Adv. Funct. Mater.*, 2020, **30**, 2003556.

4 H. Chen, Z. Shen, Z. Pan, Z. Kou, X. Liu, H. Zhang, Q. Gu, C. Guan and J. Wang, *Adv. Sci.*, 2019, **6**, 1802002.

5 L. Yu, Q. Zhu, S. Song, B. McElhenny, D. Wang, C. Wu, Z. Qin, J. Bao, Y. Yu, S. Chen and Z. Ren, *Nat. Commun.*, 2019, **10**, 5106.

6 L. Wu, F. Zhang, S. Song, M. Ning, Q. Zhu, J. Zhou, G. Gao, Z. Chen, Q. Zhou, X. Xing, T. Tong, Y. Yao, J. Bao, L. Yu, S. Chen and Z. Ren, *Adv. Mater.*, 2022, **34**, 2201774.

7 L. Yu, J. Xiao, C. Huang, Z. Zhang, M. Qiu, Y. Yu, Y. Wang and J. C. Yu, *J. Mater. Chem. A*, 2022, **10**, 17552–17560.

8 L. Wu, L. Yu, Q. Zhu, B. McElhenny, F. Zhang, C. Wu, X. Xing, J. Bao, S. Chen and Z. Ren, *Nano Energy*, 2021, **83**, 105838.

9 L. Wu, M. Ning, X. Xing, Y. Wang, F. Zhang, G. Gao, S. Song, D. Wang, C. Yuan, L. Yu, J. Bao, S. Chen and Z. Ren, *Adv. Mater.*, 2023, **35**, 2306097.